Translesion DNA synthesis-driven mutagenesis in very early embryogenesis of fast cleaving embryos

Elena Lo Furno[1], Isabelle Busseau[2], Claudio Lorenzi[3], Cima Saghira[4], Stephan Zuchner[4] and Domenico Maiorano[1*]

[1] "Genome Surveillance and Stability team" IGH, Centre National de la Recherche Scientifique, University of Montpellier, Montpellier, France.

[2] "Systemic impact des of small regulatory RNAs team" IGH, Centre National de la Recherche Scientifique, University of Montpellier, Montpellier, France.

[3] "Machine learning and gene regulation team" IGH, Centre National de la Recherche Scientifique, University of Montpellier, Montpellier, France.

[4] Department of Human Genetics, Hussman Institute for Human Genomics, University of Miami (Florida, USA)

*Correspondance

Email: domenico.maiorano@igh.cnrs.fr

Tel.: +33(0)4 34 35 99 46

Fax: +33(0)4 34 35 99 01

Abstract

In early embryogenesis of fast cleaving embryos DNA synthesis is short and surveillance mechanisms preserving genome integrity are inefficient implying the possible generation of mutations. We have analyzed mutagenesis in *Xenopus laevis* and *Drosophila melanogaster* early embryos. We report the occurrence of a high mutation rate in *Xenopus* and show that it is dependent upon the translesion DNA synthesis (TLS) master regulator Rad18. Unexpectedly, we observed a homology-directed repair contribution of Rad18 in reducing the mutation load. Genetic invalidation of TLS in the pre-blastoderm *Drosophila* embryo resulted in reduction of both the hatching rate and Single Nucleotide Variations on specific chromosome regions in adult flies. Altogether, these findings indicate that during very early *Xenopus* and *Drosophila* embryos TLS strongly contributes to the high mutation rate. This may constitute a previously unforeseen source of genetic diversity contributing to the polymorphisms of each individual with implications for genome evolution and species adaptation.

Keywords: *Xenopus*, *Drosophila*, ubiquitin, nucleus, chromatin, PCNA

Introduction

Early embryogenesis of fast cleaving embryos is characterized by unusually contracted cell cycles, made of a periodic and synchronous succession of DNA synthesis (S-phase) and mitosis with virtually absent gap phases. S-phase length is dramatically short (15 minutes in *Xenopus* and only 4 minutes in *Drosophila*) and feedback mechanisms controlling genome integrity (checkpoints) are largely repressed, as there is no time to slow down the cell cycle (*1*) for review, and references therein). These include the ATR-dependent checkpoint that monitors replication fork progression (*2*)for review). This checkpoint is activated close to the midblastula transition (MBT) in concomitance to activation of zygotic transcription (*3*–*5*). Experiments in *Xenopus* have shown that checkpoint activation is sensitive to the DNA-to-cytoplasmic ratio since it can be triggered by artificially increasing the amount of DNA in the embryo over a threshold level, a situation that mimics the increase in DNA content reached close to the MBT (*6*). Previous observations in *Caenorabditis elegans* (*7*–*9*) and more recently in *Xenopus laevis* (*10*) have implicated the translesion DNA synthesis (TLS) branch of DNA damage tolerance in silencing the DNA damage checkpoint. In *Xenopus* cleavage-stage embryos, constitutive recruitment of at least one Y-family TLS polymerase (pol η) onto replication forks, driven by the TLS master regulator Rad18 (E3) ubiquitin ligase, minimizes replication fork stalling in front of UV lesions thereby limiting ssDNA production which is essential for replication checkpoint activation (*10*–*13*). This configuration is lost prior to MBT following a developmentally-regulated decline of Rad18 abundance (*10*).

TLS pols have the unique capacity to replicate damaged DNA thanks to a catalytic site more open than that of replicative polymerases that can accommodate damaged bases. Because TLS pols cannot discriminate the insertion of the correct nucleotide and lack proofreading activity, they can be highly mutagenic especially on undamaged templates (*14*)for review). Recruitment of Y-family TLS pols (ι, η, κ and rev1) requires monoubiquitination of the replication fork-associated protein PCNA ($PCNA^{mUb}$) by Rad18 (E3) and Rad6 (E2) ubiquitin ligases complex (*15*, *16*). Aside from its TLS function, Rad18 is also implicated in error-free homology-directed DNA repair (HDR) in response to both DSBs and interstrand cross-links (*17*–*21*) . These functions are separable and lie in distinct domains of the Rad18 protein. The Rad18 TLS activity is confined to its ring finger domain (*22*), while the HDR activity mainly depends upon its zinc finger and ubiquitin binding domain (*17*, *18*). We have previously shown that in early *Xenopus* embryos PCNA is constitutively monoubiquitinated, irrespective of the presence of DNA damage (*10*). Whether TLS is active during the early embryonic cleavage stages is currently unclear. Previous work in *C. elegans* has shown that mutations in some TLS pols do not influence global mutagenesis although a *polη* and *polκ* double mutant accumulate DNA deletions (*9*). In this work, we provide evidence for TLS-dependent mutagenesis in early *Xenopus* and *Drosophila* embryos and show that in *Xenopus*, both Rad18 HDR activity and the mismatch repair system (MMR) alleviate mutagenesis, thus reducing the mutation load.

Results

High mutagenesis rate in the pre-MBT *Xenopus* embryo

We employed a classical *lacZ*-based reporter assay to measure mutagenesis in pre-MBT *Xenopus laevis* embryos. For this, a plasmid containing the whole 3 kb *lacZ* gene is microinjected in *in vitro* fertilized *Xenopus* embryos at the 2-cell stage (Figure 1A) and development is allowed to continue until before MBT (32-cell stage). Upon injection, plasmid DNAs form minichromosomes and replicate as episomes once per cell cycle with no sequence specificity (*23*, *24*). Total DNA is then extracted, purified and plasmid DNA is recovered by *E. coli* transformation, since only plasmid DNA can transform bacteria (see Materials and Methods). Bacteria are plated on a chromogenic substrate (X-gal) to screen colonies for white or blue color. Wild-type *lacZ* produces active β-galactosidase which stains colonies in blue in the presence of X-gal and IPTG, while mutations generated in the *lacZ* gene that affect β-galactosidase activity will leave colonies colorless (white) or pale blue. A pre-MBT dose of supercoiled plasmid DNA (12 ng/embryo, Figure S1A) was used in most of the experiments as previously described (*6*).

Recovery of the *lacZ*-containing plasmid DNA isolated from pre-MBT embryos into *E. coli* generated white colonies with a frequency of 0,5 %, while only a background of white colonies were observed when the plasmid was transformed in bacteria before injection (Figure 1B, pre-injection). Accordingly, mutation rate was calculated by normalization to the number of cell cycles (see materials and Methods) and estimated to be in the order of 10^{-3} (Figure 1C, *lacZ*). Importantly, the mutation rate dropped to background level when embryos were injected with a post-MBT amount of plasmid DNA. Analysis of mutations by DNA sequencing revealed the presence of both single nucleotides variations (SNVs) and unexpectedly large deletions ranging from 100 bp to 1,5 kb (Figure 1D, Figure S1B and Table SI). Mutations inspection on the *lacZ* gene showed that they are generally widespread over the entire sequence with no hotspots (Figure S1B). Analysis of the mutation spectrum shows that most SNVs detected were C>A and C>T transitions. Another frequent signature was T>A transversions, as well as nucleotides insertions and deletions. This mutation spectrum is similar to that reported for TLS pols on undamaged templates (*14*), in particular polη and polκ (*25*, *26*), although C>T transitions are also thought to be due to spontaneous deamination of 5-methyl cytosine to thymine.

The high frequency of base substitution and deletion prompted us to test the contribution of the mismatch repair system in the mutagenesis rate. For this, we overexpressed either wild-type or a catalytically inactive mutant (N38H) of Mlh1, a critical MMR component (*10*). We co-injected the *lacZ*-containing plasmid together with *in vitro*-transcribed MLH1 mRNAs to act as dominant negative by antagonizing the function of the endogenous protein (Figure 1E). While expression of $Mlh1^{WT}$ only slightly increased the mutation rate, this latter was increased 2-fold upon expression of the $Mlh1^{N38H}$ catalytically-inactive mutant (Figure 1E-G) suggesting that the MMR is functional and contributes to restrain mutagenesis. Altogether, these results show that the mutation spectrum observed in pre-MBT *Xenopus* embryos is similar to that expected for TLS pols and that mutagenesis is

restrained by the MMR system, suggesting that TLS pols may actively contribute to mutagenesis in very early embryogenesis.

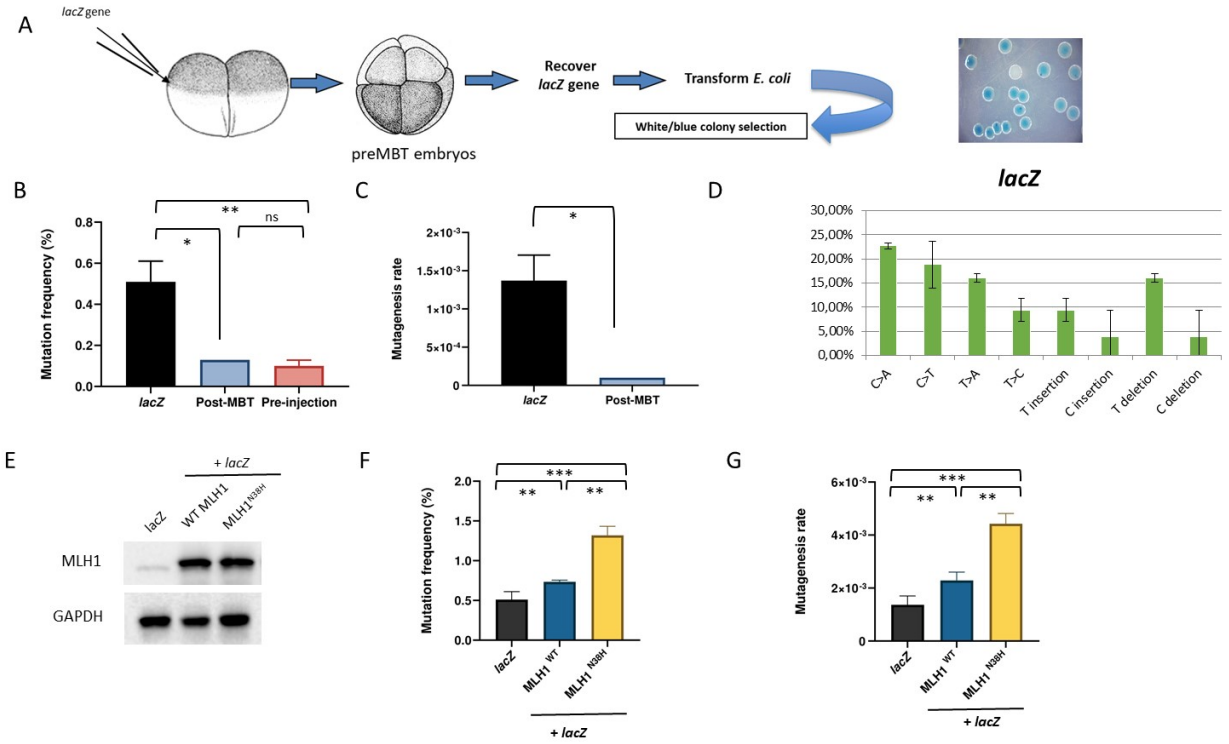

Figure 1. Pre-MBT *Xenopus* embryos accumulate polymorphisms and deletions

(A) Drawing of the experimental strategy adopted to analyze mutagenesis in *Xenopus laevis* embryos. 2-cell stage embryos are injected with a supercoiled plasmid containing *lacZ*-reporter gene (pEL1) and allowed to replicate for further 3 divisions. After embryos collection, plasmid DNA is extracted and transformed in *lacZ*-deficient bacteria for white/blue screening.

(B) Mutation frequency expressed as percentage of white colonies in each condition. The mutation frequency of *lacZ* recovered from embryos injected with a post-MBT amount of plasmid DNA is also included as comparison.

(C) Mutagenesis rate in the indicated different experimental conditions normalized to the pre-injection background values. The average of two independent experiments is shown.

(D) Mutation spectra of the *lacZ* gene recovered from *Xenopus* pre-MBT embryos after Sanger sequencing.

(E) Mutation frequency and (F) mutagenesis rate of *lacZ* isolated from *Xenopus* embryos injected as indicated.

Statistical significance was tested by unpaired Student's t test. Stars denote significant differences.* P< 0.05, ** P< 0.01, ***P <0.001, and "ns" denotes non-significant statistical test.

Rad18-dependent mutagenesis in the early *Xenopus* embryos

We have previously shown that in the pre-MBT *Xenopus* embryo TLS may be constitutively primed at replication forks in absence of external DNA damage (*10*). To determine the possible contribution of TLS to the mutagenesis in *Xenopus* embryos, we made use of a Rad18 TLS-deficient mutant in a dominant negative assay as done for Mlh1 (Figure 2A). Mutagenesis was analyzed as described in the previous paragraph. Expression of the TLS-deficient $Rad18^{C28F}$ mutant strongly reduced both the frequency of white colonies and the mutagenesis rate of about 100-fold compared to injection of $Rad18^{WT}$ or *lacZ* alone (Figure 2B-C). In contrast, $Rad18^{WT}$ overexpression did not alter the mutagenesis rate compared to embryos injected with *lacZ* plasmid only, although it generated a different mutational spectrum, consisting of predominant C insertions and T>A transversions, and remarkably no large deletions (Figure 2E and Figure S2A). T>A transversions were reported to be significantly decreased in mice bearing the $PCNA^{K164R}$ mutation that cannot support $PCNA^{mUb}$ (*27*), suggesting that this signature is Rad18 TLS activity-dependent. The residual mutagenesis observed in embryos injected with the $Rad18^{C28F}$ mutant showed a drastically reduced frequency of T>A transitions, C and T insertions, a TLS polη and polκ signature, compared to $Rad18^{WT}$ (** $p<0.05$ and 0.01 respectively), suggesting that these mutations are $PCNA^{mUb}$-dependent, while the frequency of C>T and T>C transversions increased. These latter mutations are consistent with a Rev1 signature, a TLS pol that can also be recruited independently of $PCNA^{mUb}$ (*28*, *29*).

We also tested the effect of expressing the homology-directed repair (HDR)-deficient but TLS-proficient $Rad18^{C207F}$mutant predicted to behave as $Rad18^{WT}$ (Figure 2A). Unexpectedly, however, the number of white colonies observed increased 2-fold compared to $Rad18^{WT}$ or *lacZ* alone, and the mutagenesis rate increased accordingly (Figure 2C-D) notwithstanding a similar expression level (Figure 2D). Compared to $Rad18^{WT}$, expression of this mutant produced a reduction in C>A and T>G transversions, T>A transitions and C insertions, strongly increased C>G and C>T changes (Figure 2E) and generated large deletions (Figure S2C and see below). In parallel, we analyzed mutagenesis when TLS is normally activated by UV irradiation and observed a very modest increase. The mutation spectrum showed an increase in C>A transversions and T insertions, as expected, which corresponds to TLS polη and polκ mutational signature (*25*)(Figure 2C-E and Table SI), but equally appearance of C>G and disappearance of A>G mismatches and C insertions, disappearance of C>G transitions and reduction of C>T transitions. The modest increase in UV-induced mutagenesis is expected if TLS is constitutively activated and consistent with an error-free bypass of UV lesions by TLS polη. Interestingly, no large deletions were detected (Figure S1C and see discussion). Collectively, these results show that mutagenesis in the pre-MBT *Xenopus* embryo is Rad18-dependent and that, unexpectedly, the extent of TLS-dependent mutagenesis is alleviated by the error-free Rad18-dependent HDR activity.

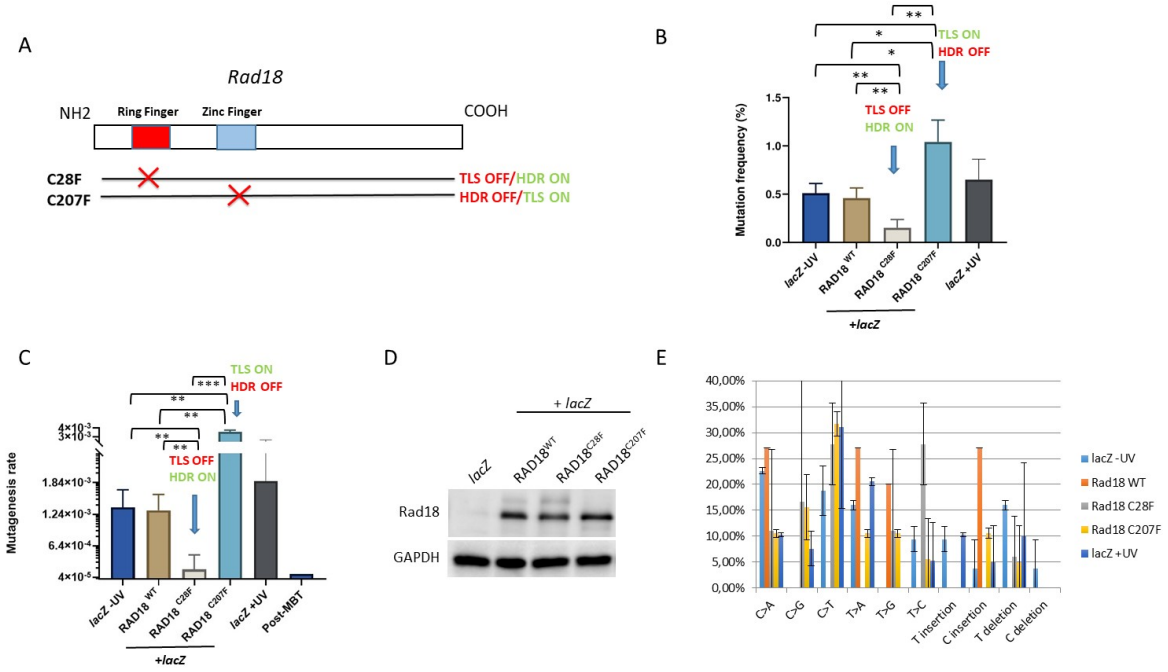

Figure 2. Differential contribution of Rad18 to mutagenesis in pre-MBT *Xenopus* embryos

(A) Schematic illustration of Rad18 domains in DNA damage tolerance and repair. TLS depends on the ring finger domain, while HDR is dependent on the zinc finger domain. The C28F mutation knocks down TLS activity (TLS OFF) while the C207F mutation knocks down HDR activity (HDR OFF).

(B) Mutation frequency and (C) mutagenesis rate of *lacZ* recovered from embryos co-injected with the indicated RAD18 mRNAs, or *lacZ* injected alone irradiated (+ UV) or not (-UV) with UV-C. The mutation frequency of *lacZ* recovered from embryos injected with a post-MBT amount of plasmid DNA (post-MBT) is also included as comparison.

(D) Western blot of total protein extracts obtained from *Xenopus* embryos subjected to the indicated experimental conditions.

(E) Mutation spectrum of *lacZ* recovered from embryos injected with the indicated RAD18 variants, or *lacZ* injected alone irradiated (+ UV) or not (-UV) with UV-C.

Statistical significance was tested by unpaired Student's t test. Stars denote significant differences:* P< 0.05, ** P< 0.01, ***P <0.001, and "ns" denotes non-significant statistical test.

Reduced hatching rate in *dpolη* maternally-deprived flies

In the aim to assess whether TLS-dependent mutagenesis is a general feature of fast cleaving embryos and to obtain genetic evidence for this process, we turned to *Drosophila melanogaster*, a more genetically amenable system compared to allotetraploid *Xenopus*. First, we wished to establish whether developmental regulation of PCNA^{mUb} also occurs during *Drosophila* embryogenesis. Similar to *Xenopus*, *Drosophila* early development occurs through

a rapid and synchronous series of embryonic cleavages before activation of zygotic transcription (MBT, Figure 3A)(*30*). Total protein extracts were prepared from *Drosophila* embryos before and after MBT and both total PCNA and PCNA^{mUb} levels were analyzed by western blot. Figure 3B-C shows that similar to what previously observed in *Xenopus* (*10*), PCNA^{mUb} is detectable in pre-MBT *Drosophila* embryos (0-2 hours) and declines at later stages (3-5 hours, post-MBT). The developmental stage where a decline in PCNA^{mUb} is observed coincided with that of Smaug, a mRNA polyadenylation factor destabilized just after MBT (*31*). We could not probe Rad18 expression since a *Drosophila* ortholog could not be found, neither by sequence homology, nor by structure-specific alignments (Busseau, Lo Furno, Bourbon, and Maiorano, unpublished).

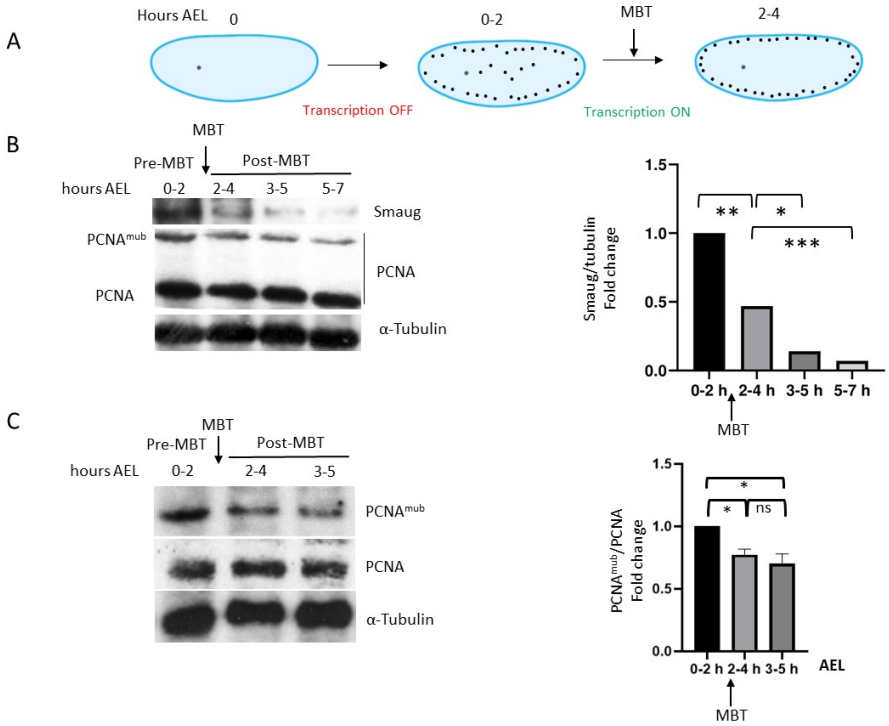

Figure 3. Developmental regulation of PCNA^{mUb} in *Drosophila*

(A) Simplified scheme of early *Drosophila melanogaster* embryogenesis. Embryos were collected at different hours after eggs laying (AEL), pre-MBT (0-2h), MBT (2-4h) and post-MBT (3-5 h and 5-7h).
(B-C) Western blot of total *Drosophila* embryos extracts analyzed at the indicated times with the indicated antibodies

(C) Right panels, quantification of western blot panels. Quantification was performed by unpaired Student's t test. Asterisks denote significant differences * P< 0.05, ** P< 0.01, ***P <0.001, and "ns" denotes non-significant statistical test.

Altogether, these observations suggest that in pre-MBT *Drosophila* embryos TLS may be constitutively primed. In line with this conclusion, previous observations have shown that *Drosophila* polη (dpolη) is highly expressed in pre-MBT embryos, localizes into interphase

nuclei, similar to what previously observed in *Xenopus* (*10*), and that *dpol*η mutant embryos are sensitive to UV-irradiation (*32*).

In *Drosophila* the presence of only three Y-family TLS pols has been reported, since a polκ ortholog could not be identified (*33*). In order to gain insight into whether TLS is also active in pre-MBT *Drosophila* embryos in the absence of external damage, and assess the consequences of this activity during development from larvae to adult stage, we employed a previously generated *dpolη*$^{Exc2.15}$null mutant (*32*). Eggs laid by females homozygous *dpolη*$^{Exc2.15}$mutant flies will be deprived of dpolη because in the pre-MBT embryos transcription is naturally shut off and is only re-established after MBT by transcription of the paternal gene provided by the sperm of wild-type flies (Figure 3A). By consequence, in this experimental setting, the observed phenotypes can be solely attributed to dpolη absence during the pre-blastoderm cleavage stages. We crossed females *dpolη*$^{Exc2.15}$ mutant flies, totally- (homozygous $^{-/-}$) or partially-deprived (heterozygous $^{+/-}$) of maternal dpolη, with isogenic wild-type males flies (Figure 4A). Development of both homozygous (maternally-depleted) and heterozygous (maternally-provided) *dpolη* flies was monitored from early embryos to adult stage and compared to that of isogenic wild-type flies. Pre-blastoderm *dpolη*$^{Exc2.15}$/ *dpolη*$^{Exc2.15}$ homozygous mutant embryos showed altered chromatin features, suggesting defects in chromosome segregation (Figure 4B). Consistent with these observations, *dpolη* maternally-deprived embryos exhibited higher mortality and reduced hatching rate compared to heterozygous embryos whose hatching rate was similar to that of the wild-type (Figure 4C). This latter result suggests that there is no dpolη dosage effect. These data are consistent with a similar phenotype very recently reported in TLS-deficient *C. elegans pcna*^{K164R} mutant embryos (*34*) and in contrast with previously published data (*32*) reporting normal hatching rate of the *dpolη*$^{Exc2.15}$/ *dpolη*$^{Exc2.15}$ mutant in absence of DNA damage. No significant difference in the survival rate was detected from larvae to adult stage in *dpolη*^{EXC215} crosses (Figure 4D). In conclusion, these results indicate that dpolη absence of before MBT affects embryo's survival from embryo to larva stage.

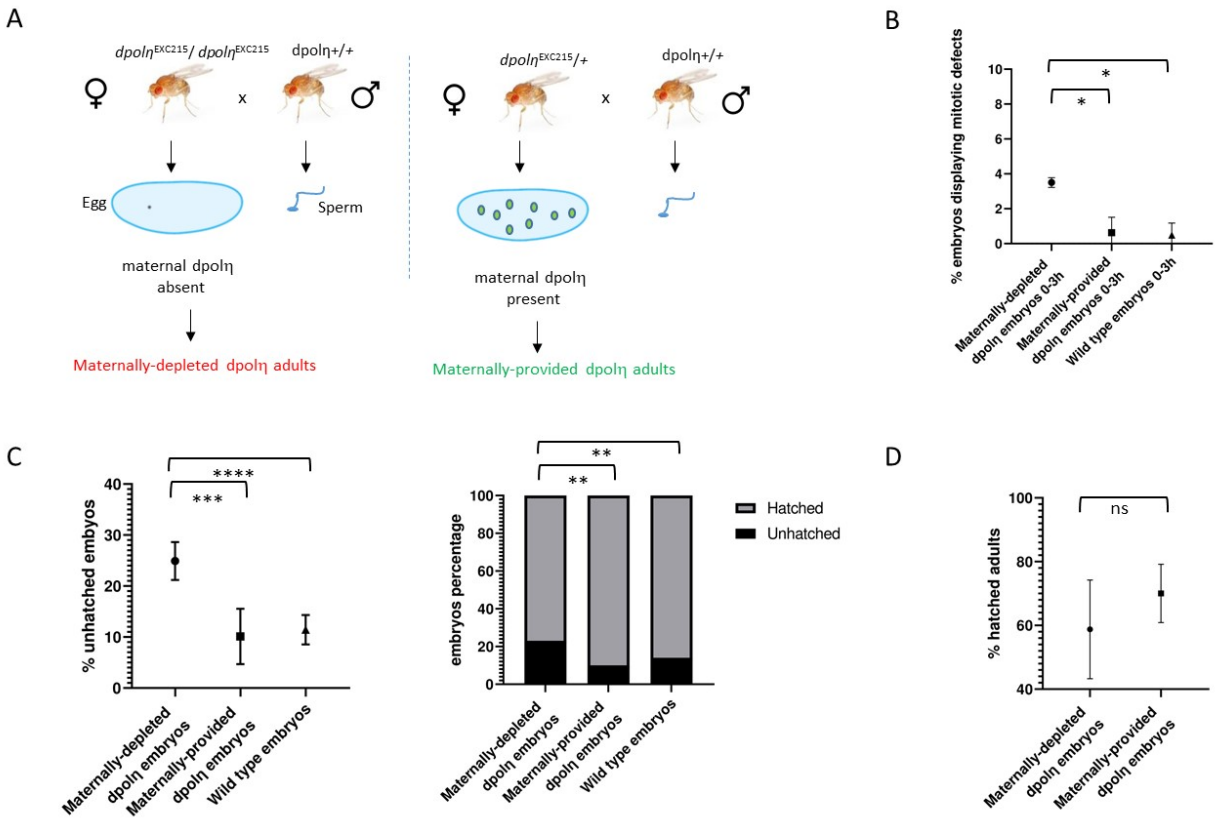

Figure 4. Absence of maternal dpolη decreases embryo's hatching rate

(A) Simplified representation of the experimental plan aimed at determining the contribution of dpolη to the mutagenesis in *Drosophila* early embryogenesis. dpolη is provided only after MBT upon zygotic gene activation.

(B) Quantification of embryos displaying mitotic defects.

(C) Statistical analysis of embryo-to-larva hatching rate of *Drosophila* embryos bearing the indicated dpolη genotypes. Embryos were collected over 12 hours and incubated at 25 °C for 2 days before calculating hatching rate. Means and standard deviation of unhatched embryos are expressed as dots and error bars in the left panel, while both unhatched and hatched embryos are represented as percentage by columns in the right panel. P values were calculating by unpaired Student's t test for the first panel (from left to right) and Fisher's exact test for the second panel.

(D) Statistical analysis (unpaired Student's t test) of larva-to-adult transition hatching rate when maternal dpolη is completely absent (homozygous maternally depleted) or partially absent (heterozygous maternally provided). Stars denote significant differences * P< 0.05, ** P< 0.01 , ***P <0.001, and "ns" denotes non-significant statistical test.

Genome-wide analysis of dpolη maternally-depleted flies

To determine the contribution of dpolη to mutagenesis specifically during the *Drosophila* cleavage stages we sequenced by Next Generation Sequencing (NGS) the whole genome of single flies described above followed by SNVs and deletions (INDELS) analysis. Due to the error-prone nature of TLS polη, especially on undamaged templates, it is expected that flies obtained from maternally-depleted *dpolη* embryos must display less mutations than heterozygous mutant flies that contain maternally-deposited dpolη in the egg and that behave similar to wild-type flies. Following alignment against the reference genome (dm6) and general genome analysis, we observed that the global number of SNVs and INDELS was not significantly reduced (Figure S3A-B), consistent with previous observations in *C. elegans* (*35*). This result can be interpreted as functional redundancy amongst Y-family TLS pols (*9*, *36*). Notwithstanding, analysis of SNVs distribution on specific chromosomes revealed a significant decrease in the frequency of SNVs in the left portion of chromosome 3 (3L, Figure 5A-C), within a cluster of Responder (Rsp) satellite DNA repeat close to pericentromeric heterochromatin (Figure 5D). The SNVs difference in this region accounts for 10-fold decrease in the mutagenesis rate in the homozygous compared to the heterozygous, consistent with an error-prone activity of dpolη. A difference was also observed in the pericentromeric region of the right part of the same chromosome (3R, Figure 5D), although the SNVs density on this latter was similar between homozygous and heterozygous, but it was shifted far from the centromere in the homozygous. Finally, a difference in SNVs distribution on chromosome Y was also observed (Figure 5E), while no variations were observed on other chromosomes (Figure S3C-E). Analysis of the mutation spectrum on chromosomes 3R and 3L (Figure 5F) revealed a predominant reduction of C>T, T>C transitions and T>A transversions. This is in line with the observation that unlike yeast and humans, dpolη misincorporates G opposite T template leading to T>C transitions (*37*).

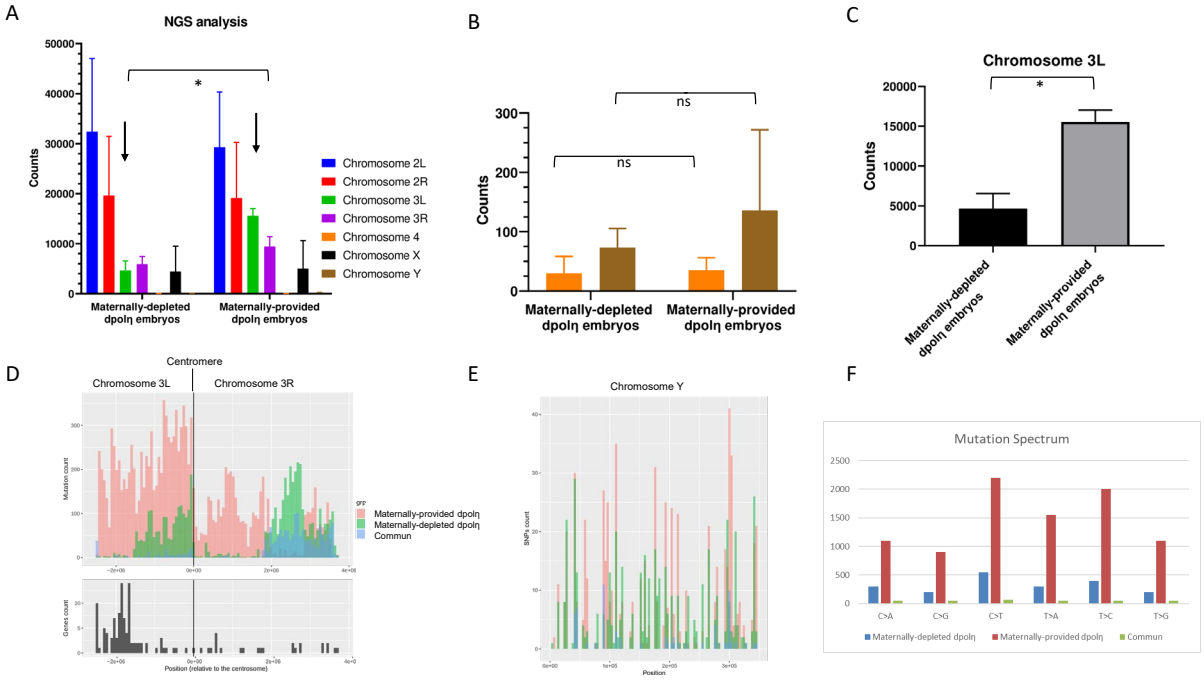

Figure 5. Chromosome-specific variation in SNVs in absence of maternal dpolη

(A-B) Analysis of SNVs rate in two independent NGS sequenced *dpolη* $^{-/-}$ and *dpolη* $^{-/+}$ maternally-deficient males adult flies. Means of variants are expressed as counts in the columns and standard deviations in the error bar (left). Right, counts difference for chromosomes 4 (orange) and Y (brown), that are not visible in panel A, are represented on an enlarged scale.

(C) Statistical analysis of SNVs counts difference on chromosome 3L in the indicated flies. Stars indicate significant differences * P< 0.05 (unpaired-two tailed Student's t test).
(D, top panel) Graphic representation of SNVs (mutation count) present in the pericentromeric region of either the left portion (3L) or right portion (3R) of chromosome 3 where a reduced genetic variation was more evident in *dpolη* $^{-/-}$ progeny. SNVs found only in either *dpolη* $^{-/-}$ or *dpolη* $^{-/+}$ progeny are shown respectively in orange or green, while common SNVs are illustrated in blue. (Bottom panel) graphic representation of genes density (genes count) along the indicated chromosome regions.

(E) SNVs distribution on chromosome Y. In these graphs, the x-axis describes the position of counted variants on this chromosome while y-axis displays how many variants were counted on that position.

(G) Graph summarizing mutation spectrum on chromosome 3L where x-axis indicates types of nucleotide variants and y-axis the quantity of counted SNVs. Unique polymorphism in either *dpolη* $^{-/-}$ or *dpolη* $^{-/+}$ progeny are separately represented in blue or in red, while mutual variants are displayed in green.

Because approximately two third of the genes located on 3L centromeric heterochromatin are required for developmental viability and/or adult fertility (*38*) we evaluated the predicted effects of mutations in *dpolh* $^{-/-}$ and *dpolh* $^{-/+}$ adults by attributing variant effect predictor (VEP) score to each variation. As a comparison, we performed the same analysis on the 3R arm of the same chromosome. VEP score determines the effect of variants (SNVs, insertions, deletions, CNVs or structural variants) on genes, transcripts, and protein sequence, as well as regulatory regions. In both *dpolh* $^{-/-}$ and d*polη* $^{-/+}$ flies genomes, the majority of variants present a modifier score more enriched in the *dpolη* $^{-/-}$ homozygous mutant on chromosome 3L compared to 3R (Figure S4A, E). Most variants in this category affect intron splicing or noncoding regions (intergenic variants, Figure S4B, F). However, once the VEP score modifier removed, the most recurrent SNVs in the *dpolη* $^{-/-}$ 3L region presented a moderate score or a low score, although we could observe a small proportion of SNVs presenting a high score specifically on this chromosome arm (Figure S2C, G). The consequences of these variants were scored and, as shown in Figure S2D, H, they lead to missense mutations in coding genes enriched in the 3R chromosome arm in the *dpolη* $^{-/-}$ mutant. This category of variants changes the genetic code, which may potentially alter the function of a protein.

Taken altogether, these data show that *dpolη* maternally-depleted adults are characterized by decreased mutations on specific chromosomes regions that probably depend upon dpolη for efficient replication during the very fast cleavage stages and containing genes important from embryos viability (*38*).

Discussion

High mutagenesis in the pre-MBT *Xenopus* embryo

In this work, we have provided evidence for the occurrence of a surprisingly high mutation rate in the very early, pre-MBT *Xenopus* embryo. Mutation rate was estimated to be in the range of 10^{-3} and corresponds to 0.8 mutations per cell cycle, a value very close to that observed in the human germline (0.4-1.2) (*39*) but slightly lower than that estimated for pre-implantation human embryos (2.8) (*40*). This mutation rate is within the range observed for Y-family TLS pols and was greatly reduced upon expression of the TLS-deficient $Rad18^{C28F}$ mutant. The corresponding mutation spectrum is also consistent with the mutagenesis spectrum of TLS pols on undamaged DNA templates. Collectively, these findings indicate that in pre-MBT *Xenopus* embryos TLS strongly contributes to the observed mutagenesis.

The residual mutations observed in the $Rad18^{C28F}$ mutant includes C>T and C>A transversions. These mutations, that were recently reported to be also predominant in early human embryos (*40*), can be a consequence of either ribonucleotides incorporation or generated as a result of cytosine deamination into uracil, which is then turned into a thymine upon replication. The concentration of ribonucleotides exceeds of about 1000-fold that of desoxyribonucleotides, and we have observed a high level of ribonucleotides incorporation during DNA synthesis in *Xenopus* egg extracts that depends upon the DNA-to-cytoplasmic ratio (Figure S2D). Ribonucleotides incorporation may be a consequence of constitutive TLS activity, in line with evidence demonstrating ribonucleotides incorporation *in vitro* by human polη (*41*, *42*). Because ribonucleotides slow down DNA replication, constitutive TLS activation facilitates their bypass, a strategy that the *Xenopus* embryos may have evolved to cope with a very contracted cell cycle. Notwithstanding, it cannot be excluded that these mutations might be also a consequence of unproofed errors of replicative DNA polymerases.

Unexpectedly, we have also observed large deletions in the *lacZ* gene recovered from pre-MBT embryos. These rearrangements are unlikely to be an artifact of the plasmid assay, since they were not detected neither in plasmids isolated from embryos co-injected with $Rad18^{WT}$ nor from UV-irradiated embryos. In this respect, genomic deletions have been observed in the *S* subgenome of adult *Xenopus laevis* (*43*) as well as in *Drosophila melanogaster* (*44*), suggesting that such genomic rearrangements might be naturally generated during evolution in these organisms. Although Y-family TLS pols can generate deletions, their extent is rather small (1-3 bp), implying other mechanisms. One of these can be replication fork instability, which is common in cells lacking DNA damage checkpoints (*5*, *45–47*). Replication fork collapse can also happen when repriming and template switch are inefficient. In the context of *Xenopus* early embryogenesis, the TLS-primase enzyme Primpol is not chromatin-bound (*10*), and $PCNA^{polyUb}$ necessary to activate template-switch could not

be detected in the absence of external DNA damage (Kermi and Maiorano., unpublished results), suggesting that neither repriming, nor templates switch may be active. Of note, Primpol has been reported to exert an anti-mutagenic activity in mice (*48*). Therefore, it cannot be excluded that Primpol absence from chromatin may also contribute to the high mutagenesis rate of pre-MBT *Xenopus* embryos. In sum, the occurrence of large deletions in early *Xenopus* embryos might be explained by replication fork collapse induced by occasional fork stalling in front of metabolically-induced DNA lesions (ribonucleotides, oxidized bases) and/or difficult to replicated DNA structures, probably as a consequence of suboptimal TLS activity due to limiting Rad18 levels (*10*). Consistent with this interpretation, spontaneous genomic deletions have been observed in *C. elegans* strains with reduced TLS function as a result of double strand breaks at forks arrested by endogenous DNA lesions (*35*). Rad18^{WT} overexpression would reduce fork stalling by boosting both TLS and HDR, suppress NHEJ toxic effect at collapsed replication forks and therefore reduce deletions. This scenario is in line with evidence showing that Rad18 has a negative effect on NHEJ (*49*, *50*) and that NHEJ is predominant over HDR in the early *Xenopus* embryo (*51*). Because deletions were predominantly observed upon expression of the Rad18^{C28F} TLS-deficient mutant, and to a much lesser extent upon expression of the error-free HDR-deficient Rad18^{C207F} mutant, it suggests that TLS and HDR play a major role in suppressing genomic rearrangements. Externally applied DNA damage may stimulate repriming and/or template switch by so far unclear mechanisms, thus facilitating replication fork restart, and suppressing replication fork collapse.

Functional conservation of constitutive TLS in the early embryogenesis of fast cleaving embryos

Similar to what observed in *Xenopus* (*10*), we have provided evidence for both developmental regulation of PCNA^{mUb} in *Drosophila* early embryogenesis, and TLS activity, suggesting that this process is also conserved in invertebrates. Unfortunately, a Rad18 ortholog could not be identified in *Drosophila*, and we failed to generate viable *pcna^{K164R}* / *pcna^{K164R}* mutant flies (Lo Furno, Busseau and Maiorano, unpublished) thus making not possible to analyze mutagenesis in a complete Y-family TLS-free context in *Drosophila*. Hence, it is currently unclear whether a Rad18 ortholog exists in *Drosophila*, and if does not, whether there is another E3 ligase that fulfils a similar function. Possible candidates are TRIP/Nopo, previously shown to be involved in TLS polη ubiquitination (*32*). *Drosophila* TRIP/Nopo appears not to be implicated since developmental regulated PCNA^{mUb} could be still observed in a *dnopo* null mutant (Figure S5). CRL4^{Cdt2} and RNF8 ubiquitin ligases, previously shown to contribute to PCNA^{mUb} in human cells, are potential candidates (*52*, *53*).

Detailed genome-wide analysis of SNVs in maternally-depleted *dpolη* adults revealed a reduction of SNVs in specific chromosome regions providing evidences for *in vivo* polη error-prone activity during *Drosophila* pre-MBT embryogenesis. In agreement with this hypothesis, the mutation spectrum for *dpolη* heterozygous maternally-depleted adults on the 3L chromosome corresponds to the reported incorporation errors of this polymerase on undamaged templates (*25*, *27*, *37*). A decrease in genetic variability was observed in the

pericentromeric region of chromosome 3L in addition to a change in SNVs distribution on chromosome Y. These genomic regions are heterochromatic and contain DNA repeats forming secondary structures that constitute a challenge for a canonical replication fork. In particular, reduced SNVs density in the *dpolη* homozygous mutant was observed on the α-satellite DNA of chromosome 3L that contains the largest cluster of *Responder* DNA repeats. In a contracted pre-MBT cell cycle, dpolη may be absolutely required to replicate the pericentromeric portion of chromosome 3. This hypothesis is supported by evidence showing that in somatic cells TLS polη is involved in replicating sequences forming secondary structures and common fragile (*54–56*). In absence of dpolη, either replicative polymerases, or the two others *Drosophila* Y-family TLS pols (polι and Rev1) may be less mutagenic although less efficient in replicating the pericentromeric region of chromosome 3. Due to inefficiency of the replication checkpoint in the *Drosophila* pre-blastoderm syncytium, embryos may accumulate chromosome abnormalities and undergo apoptosis at MBT (*5*), thus explaining the reduced hatching rate and chromosome abnormalities observed in the *dpolη* homozygous mutant. A similar phenotype was observed in *trip/nopo* (*32*)and Figure S5). The 3L chromosome region also contain a set of genes involved in development and viability. A great majority of SNVs in this region are predicted to generate mutations with low or moderate impact on genes functions. Accumulating mutations with low impact could represent a winning strategy to guarantee embryo development as opposed to apoptosis (*38*). Notwithstanding, we have also observed a small proportion of SNVs accumulating on this chromosome region that are predicted to generate mutations with high impact on gene functions. Hence, it cannot excluded that the phenotype observed in the *dpolη* homozygous flies may also be a consequence of mutations in essential genes.

Consequences of a high mutagenic rate in early embryogenesis: good or bad?

The occurrence of a high mutation rate in early developing embryos of fast cleaving organisms is rather surprising but somehow not completely unexpected since these embryos are characterized by a highly contracted cell cycle that does not leave enough time to allow quality control (*1*). This is probably the reason why these organisms have evolved mechanisms that reduce checkpoints efficiency, which would not be compatible with a contracted cell cycle. In this situation, the toll to pay is an increased risk of mutagenesis and genomic instability, as we have reported in this work. Several reports have highlighted the occurrence of genomic instability and mutations in early embryos (*1*) for review), a situation that is apparently compatible with normal development (*63*). These observations suggest that active protection mechanisms must be operating to reduce the mutation load in the embryo. Consistent with this possibility, mutagenesis dropped to background levels when *Xenopus* embryos were injected with a post-MBT dose of DNA, a situation the induces a cell cycle delay (*6*), suggesting that most of the mutations generated in pre-MBT embryos are corrected or eliminated at MBT, thus explaining both the low level of developmental defects and embryonic mortality. At this stage, cell cycle extension, activation of the DNA damage checkpoint and apoptosis would ensure repair and/or corrections of errors introduced during the fast cleaving stages thereby limiting the propagation of cells having gross chromosomal alterations (*5*, *57–59*). In

this work, we have unveiled that in *Xenopus*, Rad18 has a protective function through an error-free HDR activity that reduces its TLS mutagenic activity. In addition, we have shown that the MMR pathway also contributes to reduce mutagenesis in the pre-MBT embryo. However, we have shown that in *Drosophila*, mutations generated in the pre-blastoderm embryo are inherited in the adult, suggesting that protection mechanisms against genomic instability are not very stringent.

Introduction of random mutations, generated by so far unclear mechanisms, has been also recently observed in human embryos (Ju et al., 2017). This may constitute an unexpected and novel source of genetic variation contributing to genome evolution that may be advantageous for the adaptation of the species, but at the same time might be dangerous for life. For example, an overall high mutation rate may be important for pseudogenization, a process that silences the expression of pseudogenes (*60*) and be also important to adaptation to a new environment. A recent study identified several genes located on the *Drosophila* 3L chromosome involved in adaptation (*61*). In *Drosophila,* we have observed that polη mutagenic activity may be important to maintain the stability of centromeric DNA sequences in the pre-blastoderm embryo, thus being good for life. Finally, a recent report highlights the occurrence of diversity when reprogramming human somatic cells issued from different individuals into induced pluripotent stem cells (iPSCs). It was found that variation in different iPSC phenotypes, including differentiation capacity and cellular morphology, arises from genetic differences between individuals (*62*). Notwithstanding, a certain degree of mutations generated during very early embryogenesis (mosaicism) can be inherited by somatic cells and be responsible of certain genetic disease and/or set the genetic conditions for a predisposition to cancer (*63*). In the future, it will be important to explore which is the level of DNA damage inherited in the post-MBT embryo, and its contribution to the polymorphisms that characterize each individual.

Acknowledgments

We wish to thank Marcel Méchali for technical advises and J-S Hoffmann and SE Kearsey for critical reading of the manuscript. This project was supported by an ANR grant to D.M. E.L.F. was supported by a 3-year PhD fellowship from the “Ligue contre le Cancer” and 1-year fellowship from “Fondation ARC contre le cancer”.

Declaration of interests

The authors declare no competing interests.

Materials and Methods

Experiments with *Xenopus* were performed in accordance with current institutional and national regulations approved by the Minister of Research under supervision of the Departmental Direction of Population Protection (DDPP). *Xenopus* embryos were prepared by *in vitro* fertilization using standard procedures (*10*, *64*). Two-cell stage embryos were microinjected in the animal pole using a Nanoject auto oocyte injector under a stereomicroscope (2 injections of 9 nL^{-1} in one blastomer). Each embryo was injected with 12 ng (pre-MBT) or 72 ng (post-MBT) of supercoiled plasmid, undamaged or irradiated with 200 J/m^2 of UV-C with a UV-Stratalinker, and/or 5 ng of RAD18 mRNAs. Embryos were collected at 16- or 32-cell stage, according to Nieuwkoop and Faber normal tables, snap frozen in liquid nitrogen and stored at -80 °C.

Drosophila melanogaster stocks were maintained in K-Resin vials (25 X 95 mm) and polypropylene bottles (57 L X 57 W X 103 mm) inside a thermostatic room at 25 °C with alternating light and dark for an equal amount of hours per day. The *Drosophila* OreRmE BL # 25211 strain was employed as wild-type stock. The *Drosophila* TLS polη mutant *dpolη*$^{EXC215/TM3\ Sb}$ was previously described (*32*).

Plasmid DNAs

lacZ-containing plasmid (pEL1) was obtained by subcloning the *lac* operon from pBluescript into the *Spe*I-*Kpn*I restriction sites of pRU1103 vector, which contains full length *lacZ*. pEL1 was transformed and amplified in *E. coli* and purified using a standard protocol (QIAGEN) at a temperature lower or equal to 12 °C to obtain a near 100 % supercoiled DNA, as previously described (*65*). This procedure greatly minimizes DNA damage and background mutations. pCS2-MLH1 plasmid was obtained by subcloning human MLH1 cDNA from pCEP9MLH1 (*72*)), into the *BamH*I-*Xho*I restriction sites of pCS2 vector.

In vitro transcription

mRNA synthesis was performed with mMESSAGE mMACHINE kit SP6® (AM1340, Thermofisher). mRNAs were recovered by phenol-chloroform extraction and isopropanol precipitation. Following centrifugation and ethanol wash, mRNAs were dissolved in 20 μL^{-1} of RNase-free water. mRNAs quality was checked by formaldehyde gel electrophoresis.

Xenopus embryos and eggs protein extracts

An average of 20 embryos were lysed in Xb buffer (5 μL^{-1} of buffer per embryo; 100 mM KCl, 0.1 mM $CaCl_2$, 1 mM $MgCl_2$, 50 mM sucrose, 10 mM HEPES pH 7.7) supplemented with

cytochalasin (10 µg mL^{-1}), phosphatases (PhosSTOP 1X,) and proteases inhibitors (5 µg mL^{-1} Leupeptin, Pepstatin A and Aprotinin). After 10 min centrifugation at maximum speed in a benchtop centrifuge at 4 °C, cytoplasmic fraction was recovered, neutralized in an equal volume of Laemmli buffer 2X and boiled at 95 °C for 5 min. Embryos lysates were loaded on precast gradient gels (4-12 %, NuPAGE, Invitrogen). Gels were transferred to a nitrocellulose membrane for western blotting and incubated with the indicated antibodies. Interphasic *Xenopus* egg extracts were prepared and used as previously described (*12*, *67*).

Ribonucleotide incorporation assay

Upon thawing, *Xenopus* eggs extracts were supplemented with cycloheximide (250 µg mL^{-1}) and an energy regeneration system (1 mM ATP, 2 mM $MgCl_2$, 10 mM creatine kinase, 10 mM creatine phosphate). M13mp18 ssDNA was added as a template for DNA replication at the indicated concentrations in presence of α-^{32}PdCTP (3000Ci $mmol^{-1}$, Perkin Elmer). At the indicated time points half of the samples were neutralized in 10 mM EDTA, 0,5 % SDS, 200 µg mL^{-1} Proteinase K and incubated at 52 ° C for 1 hour. Samples were treated with 0.3 M NaOH at 55°C for 2 hours to digest incorporated ribonucleotides in the plasmid and loaded on 5M urea 8% acrylamide gel TBE 0,5 X urea after formamide denaturation at 55°C for 3 minutes. After migration, the gel was exposed to autoradiography.

Plasmid DNA isolation from embryos

Frozen embryos were crushed in STOP MIX supplemented with fresh Proteinase K (600 µg $µL^{-1}$). Embryos were homogenized with a tip in this solution while thawing. Immediately after, proteins digestion at 37 °C for 1 hour, total DNA was extracted as described above by phenol-chlorophorm extraction and ethanol precipitation. Recovered DNA was digested with *Dpn*I to destroy unreplicated plasmids and subsequently purified with QIAGEN gel extraction kit.

White/blue colonies selection and mutation frequency

DNA extracted from embryos was transformed in electrocompetent indicator bacteria (MBM7070 strain bearing an amber mutation in the *lacZ* gene) for white/blue screening and plated on selective petri dishes (40 µg mL^{-1} Xgal,; 200 µM IPTG). Over one thousand colonies were scored at least for each condition in each replicate. Plasmid DNA was isolated from mutant clones using a standard protocol (QIAGEN). After paired-end Sanger sequencing, polymorphisms were filtered for sequencing quality > 30 and analyzed on both strands using Geneious or Snapgene softwares. Mutation rates were estimated from the proportion of blue colonies observed (P_0). Before calculating the proportion of blue colonies observed (P_0), the basal percentage of white colonies prior to microinjection was subtracted from the percentage of white colonies in each experimental condition. The observed P_0 was substituted for P_0 to obtain the mutation rate (µ) using the following formula: µ=-ln(P_0 and normalized to the number of cell cycles before embryo collection.

Antibodies

The following antibodies were used: Gapdh (ab9484, Abcam); $Pcna^{mUb}$ Lys 164 (13439, Cell Signaling Technology); PCNA (PC10, Sigma); XlRad18 (*10*); SMAUG (*68*); Tubulin (DM1A, Sigma), Mlh1 (ab14206 Abcam).

Genetic crosses

"Virgin" females were isolated from culture bottles by anesthetizing with CO_2 and transferring to new vials. Selected males and females were incubated together in the same embryo collector (5,6 X 7,5 cm) at 25 °C where a dish filled with embryo medium (2 % ethanol, 4g L^{-1} MethylHydroxylBenzoate, 80g L^{-1} corn flour, 80g L^{-1} yeast, 10g L^{-1} agar, 30mg L^{-1} neutral red) is placed on the bottom. Quantifications of hatching rates (eggs to larvae) were determined as previously described (Merkle et al., 2009). Hatch rate is the ratio of hatched eggs to total eggs laid expressed as a percentage. Two hundred embryos were scored twice per genotype. Hatching of adult flies was estimated by calculating the percentage of larvae (counted 2-2,5 days after fertilization) developed to mature flies (counted 10 days after fertilization). P-values were determined using Fisher's exact test or unpaired Student's t test with GraphPad Prism.

DAPI staining of Drosophila embryos

Embryos collection (0-2 hours unless otherwise indicated) was carried out using standard techniques (*69*). Embryos were dechorionated in 50% bleach and fixed by shaking in a mixture of PFA 4% in PBS and heptane (1:1) for 30 minutes and the aqueous layer containing formaldehyde was removed. Embryos were devitellinised upon washing in methanol-heptane mixture (1:1) and conserved in methanol at -20 °C overnight and for up to a week. Embryos were rehydrated by sequential incubations of 10 minutes in Ethanol/PBS-T 7:3 (1X PBS + 0.1% Triton X-100), Ethanol/PBS-T 3:7 and PBS-T. Embryos were incubated for 30 minutes at room temperature in DAPI-PBS-T (1µg mL^{-1}) in the dark and rinsed three times in PBS-T. The third wash was performed overnight with mild shaking on a wheel in the dark at 4 °C. Samples were mounted in coverslips using Vectashield. Images were acquired with a Zeiss Axiovert Apotome microscope at 5X using Coolsnap HQ CDD camera (Photometrics) and processed using Omero 5.2.0 software. *P*-values were obtained using a two-tailed, unpaired Student's *t*-test.

Drosophila embryo protein lysates preparation

60 females and 10 males were incubated together inside embryo's collectors with embryo dishes for a certain number of hours according to the desired stage of embryos to be harvested. Collected embryos were gently rinsed off the medium with embryo collection buffer (Triton X-100 0,03 %; NaCl 68 mM). Embryos were removed from the medium using a brush and poured into a sieve (Falcon Cell Strainer 40 µM Nylon 352340). Harvested embryos were washed again and collected in a fresh tube (up to 50 μL^{-1} of embryos corresponding to

100 embryos). Laemmli 2X was added in ratio 1:1 in comparison to harvested volume and embryos were lysed by means of a pestle. After boiling embryo's mush at 95 °C for 5 min, chorion residues were removed by centrifugation with a benchtop centrifuge (max speed) at room temperature. Protein concentration was estimated by Amido Black staining using BSA of known concentration as a reference.

Genomic DNA extraction from single flies for Next Generation Illumina Sequencing.

Each fly was crushed with a pestle in a 1,5 mL^{-1} tube containing 170 µL of extraction buffer (Tris-HCl pH 8.0; 50mM; EDTA 50mM; SDS 1 %). Proteinase K (555 µg $µL^{-1}$) was added once the tissues had been completely grinded. After incubating 15 min at room temperature, cellular debris was removed twice by potassium acetate addition (0,83 M) and centrifugation with a bench-top centrifuge (max speed) at 4 °C for 10 min. DNA was isolated by double phenol/chloroform/isoamyl alcohol (25:24:1) extraction and ethanol precipitation overnight at -20 °C with glycogen (20 µg) followed by centrifugation at 4 °C. Precipitated DNA was washed with cold ethanol 70 %, dried at room temperature for 30 min and dissolved in water. The quality of extracted DNA (about 150 ng) was verified by agarose gel electrophoresis.

Illumina Next Generation Sequencing

Two genomic DNA samples per condition (two *dpol*$\eta^{-/-}$ and two *dpol*$\eta^{-/+}$ maternally-deficient adult males) were sequenced by Illumina NGS. After library construction and shotgun, whole *Drosophila* genomes were paired-end sequenced and assembled as previously described (*70*). Data were filtered for Genotype Quality > 35 and Depth > 10 before sequences alignment against the *Drosophila* reference genome (Flybase release 6). Data have been submitted to Gene Expression Omnibus (GEO, https://www.ncbi.nlm.nih.gov/geo/; ID GSE161335). SNVs distribution, rate and spectra in each chromosome were calculated with R software.

Statistics

Statistical analysis was performed using the Prism software (version 8) with an unpaired Student's t test. Stars indicate significant differences * P< 0.05, ** P< 0 .01, ***P <0.001, and "ns" denotes non-significant statistical test.

References

1. C. Kermi, A. Aze, D. Maiorano, Preserving Genome Integrity During the Early Embryonic DNA Replication Cycles. *Genes (Basel)*. **10** (2019), doi:10.3390/genes10050398.

2. J. C. Saldivar, D. Cortez, K. A. Cimprich, The essential kinase ATR: ensuring faithful duplication of a challenging genome. *Nat Rev Mol Cell Biol* (2017), doi:10.1038/nrm.2017.67.

3. S. A. Blythe, E. F. Wieschaus, Zygotic genome activation triggers the DNA replication checkpoint at the midblastula transition. *Cell*. **160**, 1169–81 (2015).

4. J. Newport, M. Dasso, On the coupling between DNA replication and mitosis. *Journal of cell science. Supplement*. **12**, 149–60 (1989).

5. O. C. Sibon, V. A. Stevenson, W. E. Theurkauf, DNA-replication checkpoint control at the Drosophila midblastula transition. *Nature*. **388**, 93–7 (1997).

6. C. W. Conn, A. L. Lewellyn, J. L. Maller, The DNA damage checkpoint in embryonic cell cycles is dependent on the DNA-to-cytoplasmic ratio. *Dev Cell*. **7**, 275–81 (2004).

7. A. H. Holway, S. H. Kim, A. La Volpe, W. M. Michael, Checkpoint silencing during the DNA damage response in Caenorhabditis elegans embryos. *J Cell Biol*. **172**, 999–1008 (2006).

8. T. Ohkumo, C. Masutani, T. Eki, F. Hanaoka, Deficiency of the Caenorhabditis elegans DNA polymerase eta homologue increases sensitivity to UV radiation during germ-line development. *Cell Struct Funct*. **31**, 29–37 (2006).

9. S. F. Roerink, W. Koole, L. C. Stapel, R. J. Romeijn, M. Tijsterman, A broad requirement for TLS polymerases eta and kappa, and interacting sumoylation and nuclear pore proteins, in lesion bypass during C. elegans embryogenesis. *PLoS Genet*. **8**, e1002800 (2012).

10. C. Kermi, S. Prieto, S. van der Laan, N. Tsanov, B. Recolin, E. Uro-Coste, M. B. Delisle, D. Maiorano, RAD18 Is a Maternal Limiting Factor Silencing the UV-Dependent DNA Damage Checkpoint in Xenopus Embryos. *Dev Cell*. **34**, 364–72 (2015).

11. D. Shechter, V. Costanzo, J. Gautier, ATR and ATM regulate the timing of DNA replication origin firing. *Nat Cell Biol*. **6**, 648–55 (2004).

12. B. Recolin, S. Van der Laan, D. Maiorano, Role of replication protein A as sensor in activation of the S-phase checkpoint in Xenopus egg extracts. *Nucleic Acids Res*. **40**, 3431–42 (2012).

13. C. Van, S. Yan, W. M. Michael, S. Waga, K. A. Cimprich, Continued primer synthesis at stalled replication forks contributes to checkpoint activation. *J Cell Biol*. **189**, 233–46 (2010).

14. A. Vaisman, R. Woodgate, Translesion DNA polymerases in eukaryotes: what makes them tick? *Crit. Rev. Biochem. Mol. Biol.* **52**, 274–303 (2017).

15. P. L. Kannouche, J. Wing, A. R. Lehmann, Interaction of human DNA polymerase eta with monoubiquitinated PCNA: a possible mechanism for the polymerase switch in response to DNA damage. *Mol Cell*. **14**, 491–500 (2004).

16. K. Watanabe, S. Tateishi, M. Kawasuji, T. Tsurimoto, H. Inoue, M. Yamaizumi, Rad18 guides poleta to replication stalling sites through physical interaction and PCNA monoubiquitination. *EMBO J*. **23**, 3886–96 (2004).

17. J. Huang, M. S. Huen, H. Kim, C. C. Leung, J. N. Glover, X. Yu, J. Chen, RAD18 transmits DNA damage signalling to elicit homologous recombination repair. *Nat Cell Biol*. **11**, 592–603 (2009).

18. K. Watanabe, K. Iwabuchi, J. Sun, Y. Tsuji, T. Tani, K. Tokunaga, T. Date, M. Hashimoto, M. Yamaizumi, S. Tateishi, RAD18 promotes DNA double-strand break repair during G1 phase through chromatin retention of 53BP1. *Nucleic Acids Res*. **37**, 2176–93 (2009).

19. C. M. Helchowski, L. F. Skow, K. H. Roberts, C. L. Chute, C. E. Canman, A small ubiquitin binding domain inhibits ubiquitin-dependent protein recruitment to DNA repair foci. *Cell Cycle*. **12** (2013) (available at http://www.ncbi.nlm.nih.gov/pubmed/24107634).

20. D. M. Moquin, M.-M. Genois, J.-M. Zhang, J. Ouyang, T. Yadav, R. Buisson, S. A. Yazinski, J. Tan, M. Boukhali, J.-P. Gagné, G. G. Poirier, L. Lan, W. Haas, L. Zou, Localized protein biotinylation at DNA damage sites identifies ZPET, a repressor of homologous recombination. *Genes Dev.* **33**, 75–89 (2019).

21. M. Raschle, G. Smeenk, R. K. Hansen, T. Temu, Y. Oka, M. Y. Hein, N. Nagaraj, D. T. Long, J. C. Walter, K. Hofmann, Z. Storchova, J. Cox, S. Bekker-Jensen, N. Mailand, M. Mann, DNA repair. Proteomics reveals dynamic assembly of repair complexes during bypass of DNA cross-links. *Science (New York, N.Y.)*. **348**, 1253671 (2015).

22. S. Tateishi, Y. Sakuraba, S. Masuyama, H. Inoue, M. Yamaizumi, Dysfunction of human Rad18 results in defective postreplication repair and hypersensitivity to multiple mutagens. *Proceedings of the National Academy of Sciences of the United States of America*. **97**, 7927–32 (2000).

23. M. Mechali, R. M. Harland, DNA synthesis in a cell-free system from Xenopus eggs: priming and elongation on single-stranded DNA in vitro. *Cell*. **30**, 93–101 (1982).

24. M. Mechali, S. Kearsey, Lack of specific sequence requirement for DNA replication in Xenopus eggs compared with high sequence specificity in yeast. *Cell*. **38**, 55–64 (1984).

25. T. Matsuda, K. Bebenek, C. Masutani, F. Hanaoka, T. A. Kunkel, Low fidelity DNA synthesis by human DNA polymerase-eta. *Nature*. **404**, 1011–3 (2000).

26. T. Ogi, T. Kato, T. Kato, H. Ohmori, Mutation enhancement by DINB1, a mammalian homologue of the Escherichia coli mutagenesis protein dinB. *Genes Cells*. **4**, 607–618 (1999).

27. P. Langerak, A. O. H. Nygren, P. H. L. Krijger, P. C. M. van den Berk, H. Jacobs, A/T mutagenesis in hypermutated immunoglobulin genes strongly depends on PCNAK164 modification. *J. Exp. Med.* **204**, 1989–1998 (2007).

28. C. E. Edmunds, L. J. Simpson, J. E. Sale, PCNA ubiquitination and REV1 define temporally distinct mechanisms for controlling translesion synthesis in the avian cell line DT40. *Molecular cell*. **30**, 519–29 (2008).

29. C. Guo, P. L. Fischhaber, M. J. Luk-Paszyc, Y. Masuda, J. Zhou, K. Kamiya, C. Kisker, E. C. Friedberg, Mouse Rev1 protein interacts with multiple DNA polymerases involved in translesion DNA synthesis. *The EMBO journal*. **22**, 6621–30 (2003).

30. J. A. Farrell, P. H. O'Farrell, From egg to gastrula: how the cell cycle is remodeled during the Drosophila mid-blastula transition. *Annual review of genetics*. **48**, 269–94 (2014).

31. B. Benoit, C. H. He, F. Zhang, S. M. Votruba, W. Tadros, J. T. Westwood, C. A. Smibert, H. D. Lipshitz, W. E. Theurkauf, An essential role for the RNA-binding protein Smaug during the Drosophila maternal-to-zygotic transition. *Development (Cambridge, England)*. **136**, 923–32 (2009).

32. H. A. Wallace, J. A. Merkle, M. C. Yu, T. G. Berg, E. Lee, G. Bosco, L. A. Lee, TRIP/NOPO E3 ubiquitin ligase promotes ubiquitylation of DNA polymerase eta. *Development*. **141**, 1332–41 (2014).

33. S. J. Marygold, H. Attrill, E. Speretta, K. Warner, M. Magrane, M. Berloco, S. Cotterill, M. McVey, Y. Rong, M. Yamaguchi, The DNA polymerases of *Drosophila melanogaster*. *Fly*, 1–13 (2020).

34. Z. Shao, S. Niwa, A. Higashitani, Y. Daigaku, Vital roles of PCNA K165 modification during C. elegans gametogenesis and embryogenesis. *DNA Repair (Amst.)*. **82**, 102688 (2019).

35. S. F. Roerink, R. van Schendel, M. Tijsterman, Polymerase theta-mediated end joining of replication-associated DNA breaks in C. elegans. *Genome Res.* **24**, 954–962 (2014).

36. J. G. Jansen, P. Temviriyanukul, N. Wit, F. Delbos, C.-A. Reynaud, H. Jacobs, N. de Wind, Redundancy of mammalian Y family DNA polymerases in cellular responses to genomic DNA lesions induced by ultraviolet light. *Nucleic Acids Res.* **42**, 11071–11082 (2014).

37. T. Ishikawa, N. Uematsu, T. Mizukoshi, S. Iwai, H. Iwasaki, C. Masutani, F. Hanaoka, R. Ueda, H. Ohmori, T. Todo, Mutagenic and nonmutagenic bypass of DNA lesions by Drosophila DNA polymerases dpoleta and dpoliota. *The Journal of biological chemistry*. **276**, 15155–63 (2001).

38. M. Syrzycka, G. Hallson, K. A. Fitzpatrick, I. Kim, S. Cotsworth, R. E. Hollebakken, K. Simonetto, L. Yang, S. Luongo, K. Beja, A. B. Coulthard, A. J. Hilliker, D. A. Sinclair, B. M. Honda, Genetic and Molecular Analysis of Essential Genes in Centromeric Heterochromatin of the Left Arm of Chromosome 3 in Drosophila melanogaster. *G3 (Bethesda)*. **9**, 1581–1595 (2019).

39. R. Rahbari, A. Wuster, S. J. Lindsay, R. J. Hardwick, L. B. Alexandrov, S. A. Turki, A. Dominiczak, A. Morris, D. Porteous, B. Smith, M. R. Stratton, UK10K Consortium, M. E. Hurles, Timing, rates and spectra of human germline mutation. *Nat. Genet.* **48**, 126–133 (2016).

40. Y. S. Ju, I. Martincorena, M. Gerstung, M. Petljak, L. B. Alexandrov, R. Rahbari, D. C. Wedge, H. R. Davies, M. Ramakrishna, A. Fullam, S. Martin, C. Alder, N. Patel, S. Gamble, S. O'Meara, D. D. Giri, T. Sauer, S. E. Pinder, C. A. Purdie, Å. Borg, H. Stunnenberg, M. van de Vijver, B. K. T. Tan, C. Caldas, A. Tutt, N. T. Ueno, L. J. van 't Veer, J. W. M. Martens, C. Sotiriou, S. Knappskog, P. N. Span, S. R. Lakhani, J. E. Eyfjörd, A.-L. Børresen-Dale, A. Richardson, A. M. Thompson, A. Viari, M. E. Hurles, S. Nik-Zainal, P. J. Campbell, M. R. Stratton, Somatic mutations reveal asymmetric cellular dynamics in the early human embryo. *Nature*. **543**, 714–718 (2017).

41. E. Mentegari, E. Crespan, L. Bavagnoli, M. Kissova, F. Bertoletti, S. Sabbioneda, R. Imhof, S. J. Sturla, A. Nilforoushan, U. Hübscher, B. van Loon, G. Maga, Ribonucleotide incorporation by human DNA polymerase η impacts translesion synthesis and RNase H2 activity. *Nucleic Acids Res.* **45**, 2600–2614 (2017).

42. Y. Su, M. Egli, F. P. Guengerich, Mechanism of Ribonucleotide Incorporation by Human DNA Polymerase η. *J. Biol. Chem.* **291**, 3747–3756 (2016).

43. A. M. Session, Y. Uno, T. Kwon, J. A. Chapman, A. Toyoda, S. Takahashi, A. Fukui, A. Hikosaka, A. Suzuki, M. Kondo, S. J. van Heeringen, I. Quigley, S. Heinz, H. Ogino, H. Ochi, U. Hellsten, J. B.

Lyons, O. Simakov, N. Putnam, J. Stites, Y. Kuroki, T. Tanaka, T. Michiue, M. Watanabe, O. Bogdanovic, R. Lister, G. Georgiou, S. S. Paranjpe, I. van Kruijsbergen, S. Shu, J. Carlson, T. Kinoshita, Y. Ohta, S. Mawaribuchi, J. Jenkins, J. Grimwood, J. Schmutz, T. Mitros, S. V. Mozaffari, Y. Suzuki, Y. Haramoto, T. S. Yamamoto, C. Takagi, R. Heald, K. Miller, C. Haudenschild, J. Kitzman, T. Nakayama, Y. Izutsu, J. Robert, J. Fortriede, K. Burns, V. Lotay, K. Karimi, Y. Yasuoka, D. S. Dichmann, M. F. Flajnik, D. W. Houston, J. Shendure, L. DuPasquier, P. D. Vize, A. M. Zorn, M. Ito, E. M. Marcotte, J. B. Wallingford, Y. Ito, M. Asashima, N. Ueno, Y. Matsuda, G. J. C. Veenstra, A. Fujiyama, R. M. Harland, M. Taira, D. S. Rokhsar, Genome evolution in the allotetraploid frog Xenopus laevis. *Nature*. **538**, 336–343 (2016).

44. D. A. Petrov, D. L. Hartl, High rate of DNA loss in the Drosophila melanogaster and Drosophila virilis species groups. *Mol Biol Evol*. **15**, 293–302 (1998).

45. H. Dungrawala, K. L. Rose, K. P. Bhat, K. N. Mohni, G. G. Glick, F. B. Couch, D. Cortez, The Replication Checkpoint Prevents Two Types of Fork Collapse without Regulating Replisome Stability. *Molecular Cell*. **59**, 998–1010 (2015).

46. R. D. Paulsen, K. A. Cimprich, The ATR pathway: fine-tuning the fork. *DNA Repair (Amst.)*. **6**, 953–966 (2007).

47. O. C. Sibon, A. Laurençon, R. Hawley, W. E. Theurkauf, The Drosophila ATM homologue Mei-41 has an essential checkpoint function at the midblastula transition. *Curr. Biol.* **9**, 302–312 (1999).

48. B. Pilzecker, O. A. Buoninfante, C. Pritchard, O. S. Blomberg, I. J. Huijbers, P. C. M. van den Berk, H. Jacobs, PrimPol prevents APOBEC/AID family mediated DNA mutagenesis. *Nucleic Acids Res.* **44**, 4734–4744 (2016).

49. S. Kobayashi, Y. Kasaishi, S. Nakada, T. Takagi, S. Era, A. Motegi, R. K. Chiu, S. Takeda, K. Hirota, Rad18 and Rnf8 facilitate homologous recombination by two distinct mechanisms, promoting Rad51 focus formation and suppressing the toxic effect of nonhomologous end joining. *Oncogene*. **34**, 4403–11 (2015).

50. A. Saberi, H. Hochegger, D. Szuts, L. Lan, A. Yasui, J. E. Sale, Y. Taniguchi, Y. Murakawa, W. Zeng, K. Yokomori, T. Helleday, H. Teraoka, H. Arakawa, J. M. Buerstedde, S. Takeda, RAD18 and poly(ADP-ribose) polymerase independently suppress the access of nonhomologous end joining to double-strand breaks and facilitate homologous recombination-mediated repair. *Molecular and cellular biology*. **27**, 2562–71 (2007).

51. C. W. Lehman, M. Clemens, D. K. Worthylake, J. K. Trautman, D. Carroll, Homologous and illegitimate recombination in developing Xenopus oocytes and eggs. *Molecular and Cellular Biology*. **13**, 6897–6906 (1993).

52. K. Terai, T. Abbas, A. A. Jazaeri, A. Dutta, CRL4(Cdt2) E3 ubiquitin ligase monoubiquitinates PCNA to promote translesion DNA synthesis. *Mol Cell*. **37**, 143–9 (2010).

53. S. Zhang, Y. Zhou, A. Sarkeshik, J. R. Yates 3rd, T. M. Thomson, Z. Zhang, E. Y. Lee, M. Y. Lee, Identification of RNF8 as a ubiquitin ligase involved in targeting the p12 subunit of DNA polymerase delta for degradation in response to DNA damage. *J Biol Chem*. **288**, 2941–50 (2013).

54. V. Bergoglio, A. S. Boyer, E. Walsh, V. Naim, G. Legube, M. Y. Lee, L. Rey, F. Rosselli, C. Cazaux, K. A. Eckert, J. S. Hoffmann, DNA synthesis by Pol eta promotes fragile site stability by preventing under-replicated DNA in mitosis. *J Cell Biol*. **201**, 395–408 (2013).

55. R. Betous, L. Rey, G. Wang, M. J. Pillaire, N. Puget, J. Selves, D. S. Biard, K. Shin-ya, K. M. Vasquez, C. Cazaux, J. S. Hoffmann, Role of TLS DNA polymerases eta and kappa in processing naturally occurring structured DNA in human cells. *Mol Carcinog*. **48**, 369–78 (2009).

56. L. Rey, J. M. Sidorova, N. Puget, F. Boudsocq, D. S. Biard, R. J. Monnat Jr., C. Cazaux, J. S. Hoffmann, Human DNA polymerase eta is required for common fragile site stability during unperturbed DNA replication. *Mol Cell Biol*. **29**, 3344–54 (2009).

57. J. A. Anderson, A. L. Lewellyn, J. L. Maller, Ionizing radiation induces apoptosis and elevates cyclin A1-Cdk2 activity before but not after the midblastula transition in Xenopus. *Mol Biol Cell*. **8**, 1195–206 (1997).

58. H. Bolton, S. J. L. Graham, N. Van der Aa, P. Kumar, K. Theunis, E. Fernandez Gallardo, T. Voet, M. Zernicka-Goetz, Mouse model of chromosome mosaicism reveals lineage-specific depletion of aneuploid cells and normal developmental potential. *Nat Commun*. **7**, 11165 (2016).

59. C. Hensey, J. Gautier, A developmental timer that regulates apoptosis at the onset of gastrulation. *Mech Dev*. **69**, 183–95 (1997).

60. A. Force, M. Lynch, F. B. Pickett, A. Amores, Y. L. Yan, J. Postlethwait, Preservation of duplicate genes by complementary, degenerative mutations. *Genetics*. **151**, 1531–1545 (1999).

61. L. Mateo, G. E. Rech, J. González, Genome-wide patterns of local adaptation in Western European Drosophila melanogaster natural populations. *Scientific Reports*. **8**, 16143 (2018).

62. H. Kilpinen, A. Goncalves, A. Leha, V. Afzal, K. Alasoo, S. Ashford, S. Bala, D. Bensaddek, F. P. Casale, O. J. Culley, P. Danecek, A. Faulconbridge, P. W. Harrison, A. Kathuria, D. McCarthy, S. A. McCarthy, R. Meleckyte, Y. Memari, N. Moens, F. Soares, A. Mann, I. Streeter, C. A. Agu, A. Alderton, R. Nelson, S. Harper, M. Patel, A. White, S. R. Patel, L. Clarke, R. Halai, C. M. Kirton, A. Kolb-Kokocinski, P. Beales, E. Birney, D. Danovi, A. I. Lamond, W. H. Ouwehand, L. Vallier, F. M. Watt, R. Durbin, O. Stegle, D. J. Gaffney, Common genetic variation drives molecular heterogeneity in human iPSCs. *Nature*. **546**, 370–375 (2017).

63. R. P. Erickson, Recent advances in the study of somatic mosaicism and diseases other than cancer. *Current Opinion in Genetics & Development*. **26**, 73–78 (2014).

64. H. L. Sivel Grainer, R. M. ,. Harland, R. M., *Early Development of Xenopus laevis. A laboratory manual.* (Cold Spring harbour Laboratory Press, New York, 2000).

65. A. Carbone, F. M. Fioretti, L. Fucci, J. Ausió, M. Piscopo, High efficiency method to obtain supercoiled DNA with a commercial plasmid purification kit. *Acta Biochim. Pol.* **59**, 275–278 (2012).

66. N. Papadopoulos, N. Nicolaides, Y. Wei, S. Ruben, K. Carter, C. Rosen, W. Haseltine, R. Fleischmann, C. Fraser, M. Adams, al. et, Mutation of a mutL homolog in hereditary colon cancer. *Science*. **263**, 1625–1629 (1994).

67. A. W. Murray, Cell cycle extracts. *Methods in Cell Biology*. **36**, 581–605 (1991).

68. A. Chartier, P. Klein, S. Pierson, N. Barbezier, T. Gidaro, F. Casas, S. Carberry, P. Dowling, L. Maynadier, M. Bellec, M. Oloko, C. Jardel, B. Moritz, G. Dickson, V. Mouly, K. Ohlendieck, G. Butler-Browne, C. Trollet, M. Simonelig, Mitochondrial dysfunction reveals the role of mRNA poly(A) tail regulation in oculopharyngeal muscular dystrophy pathogenesis. *PLoS Genet.* **11**, e1005092 (2015).

69. W. F. Rothwell, W. Sullivan, in *Drosphila protocols* (Cold Spring Harbor laboratory Press, Cold Spring Harbor, New York (USA), W. Sullivan, M. Ashburner and R.S. Hawley., 2000), pp. 141–157.

70. M. A. Gonzalez, D. Van Booven, W. Hulme, R. H. Ulloa, R. F. A. Lebrigio, J. Osterloh, M. Logan, M. Freeman, S. Zuchner, Whole Genome Sequencing and a New Bioinformatics Platform Allow for Rapid Gene Identification in D. melanogaster EMS Screens. *Biology (Basel)*. **1**, 766–777 (2012).